Novel Oligo(9,10-anthrylene)s: Models for Electron Transfer and High-Spin Formation

Uwe Müller and Martin Baumgarten*

Contribution from the Max-Planck-Institut für Polymerforschung, Ackermannweg 10, D-55128 Mainz, Federal Republic Germany

Received February 24, 1995[⊗]

Abstract: Newly synthesized soluble oligo(9,10-anthrylene)s **1** have been subjected to reduction with alkali metal. The electron paramagnetic resonance/electron nuclear double resonance (EPR/ENDOR) studies of corresponding dimer, trimer, and tetramer monoradicals demonstrate that the rate of intramolecular electron transfer between anthracene moieties sensitively depends on the special substitution pattern and the ion pair structure. These features allow for a switching from effectively delocalized to localized states. In agreement with theoretical investigations, high-spin formation of the higher charged species has been obtained. The maximum spin multiplicity received so far is a quintet state for the tetraanion of the tetraanthrylene. The stability of the highly charged states is proven by NMR spectroscopic investigations, where a completely reduced diamagnetic hexaanion of trianthrylene has been characterized by ^{1}H and ^{13}C NMR. As revealed by temperature dependent EPR measurement of the dimer dianion, the triplet state is thermally excited (signal intensity reaches a maximum at 20 K) and the zero-field splitting loses its axial character (typical for orthogonal alignment) at low temperatures, pointing to increased orthorhombicity with decreasing temperature (100-10 K). Although the ground state is singlet, the energy of the triplet state lies only 60 cal/mol above that of the singlet. Surprisingly also the higher spin states of the oligomers were found to be thermally activated with 120 cal/mol for the doublet-quartet ($S = 3/2$) transition and 180 cal/mol for the quintet−singlet ($S = 2$) transition.

1. Introduction

There has been much recent interest in the design of organic materials which are suited for electron transfer and electron storage.[1−3] In this context, biaryls, oligoarylenes, and polyarylenes serve as important chromophores and electrophores.[4,5] Their electronic properties depend sensitively upon interring conjugation. Sufficient conjugative interaction is expected to create a single extended π-system with a drastically lowered HOMO−LUMO energy gap, while interruption of conjugation by strong steric hindrance or use of saturated bridges leads to an electronically uncoupled π-subunit.[6] Upon charging, the extended π-systems should give rise to a complete charge delocalization described by a single minimum potential, while conjugatively hindered molecules should exhibit a double or multiple minimum potential, where the charge distribution depends on the kinetics of an electron transfer between the potential minima. The differentiation of conjugation in bridged electrophores has led to the classification of multielectrophoric materials into conducting polymers and redox polymers.[2,7]

An important aspect in the redox behavior of bis- and polyelectrophoric systems with vanishing conjugative interaction of π-subunits concerns the possibility of intramolecular electron-hopping processes upon photoexcitation or upon thermal activation of a monocharged state.[8,9] In contrast to intramolecular electron transfer reactions between suitable donor and acceptor functions, the electron exchange between identical electrophores is a degenerate process.

It appears that the rate of intramolecular charge transfer and the observed spin-density distribution for biselectrophoric redox systems over one or two units depend upon (i) the overall reorganization energy and thus the nature of the subunits, (ii) the way in which the subunits are linked, and (iii) the ion pairing.[1] Another factor controlling the electron transfer is the number of extra charges since successive reduction to di-, tri-, or even tetraanions affects not only the prevailing ion pair structure but also the spin multiplicity of the species and the relative spatial arrangement of the subunits.[10,11] These empirical findings should allow for a control of the rate of electron transfer processes by creating the appropriate structural and experimental conditions.

For charge storage purposes, a conjugation barrier with nearly independent redox active behavior of the subunits and high density of localized charges is particularly favorable.

Vanishing conjugative interaction of π-units and, thus, strongly inhibited spin−spin pairing, on the other hand, also occur in organic high-spin systems, which play a central role in the search for organic ferromagnets.[12] Consequently, materials which are suited for effective charge storage may also be

[⊗] Abstract published in *Advance ACS Abstracts,* May 1, 1995.

(1) Baumgarten, M.; Huber, W.; Müllen, K. *Adv. Phys. Org. Chem.* **1992**, *28*, 1.

(2) Bohnen, A.; Räder, J.; Müllen, K. *Synth. Met.* **1992**, *47*, 37.

(3) Baumgarten, M.; Müller, U.; Müllen, K. *AIP Conf. Proc. Ser., St. Thomas* **1992**, *68*.

(4) Naarmann, H. *Angew. Makromol. Chem.* **1982**, *109/110*, 295.

(5) (a) Baumgarten, M.; Müllen, K. *Top. Curr. Chem.* **1994**, *169*, 1. (b) Müllen, K. *Pure Appl. Chem.* **1993**, *65*, 89. (c) Müller, U.; Adam, M.; Müllen, K. *Chem. Ber.* **1994**, *127*, 437. (d) Müller, U.; Mangel, T.; Müllen, K. *Macromol. Rapid Commun.* **1994**, *115*, 45.

(6) (a) Koch, K.-H.; Müllen, K. *Chem. Ber.* **1991**, *124*, 2091. (b) Bohnen, A.; Koch, K.-H.; Lüttke, W.; Müllen, K. *Angew. Chem., Int. Ed. Eng.* **1990**, *29*, 525. (c) Becker, B.; Bohnen, A.; Ehrenfreund, M.; Wohlfarth, W.; Sakata, Y.; Huber, W.; Müllen, K. *J. Am. Chem. Soc.* **1991**, *113*, 1121.

(7) (a) Wegner, G. *Angew. Chem., Int. Ed. Engl.* **1981**, *20*, 361. (b) Heinze, J. *Top. Curr. Chem.* **1990**, *152*, 1.

(8) (a) Mazur, S.; Dixit, V. M.; Gerson, F. *J. Am. Chem. Soc.* **1980**, *102*, 5343. (b) Farazdel, A.; Dupuis, M.; Clementi, E.; Aviram, A. *J. Am. Chem. Soc.* **1990**, *112*, 4206.

(9) (a) Miller, J. R.; Calcaterra, L. T.; Closs, G. L. *J. Am. Chem. Soc.* **1984**, *106*, 3047. (b) Liang, N.; Miller, J. R.; Closs, G. L. *J. Am. Chem. Soc.* **1990**, *112*, 5353.

(10) Fiedler, J.; Huber, W.; Müllen, K. *Angew. Chem., Int. Ed. Engl.* **1986**, *25*, 443.

(11) Closs, G. L.; Piotrowiak, P.; MacInnes, J. M.; Flemming, G. R. *J. Am. Chem. Soc.* **1988**, *110*, 2652.

0002-7863/95/1517-5840$09.00/0

Chart 1

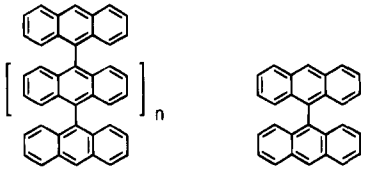

1 2

candidates for high-spin states. While the unpairing of individual spins has usually been sought in π-conjugated compounds with so-called "non-Kekulé" structures,[12,13] recent approaches toward high-spin molecules include the almost orthogonal alignment of spin-carrying subunits.[14-16]

In that respect, oligo(9,10-anthrylene)s **1** (Chart 1) seem to be especially promising, because they combine a more or less perpendicular arrangement of the subunits with a high redox activity of the individual building blocks. In agreement with earlier theoretical studies,[15,16] we have been able to show that ferromagnetic coupling should be possible in the triplet dianion of **2** and in the polyanions of poly(9,10-anthrylene) (**1**) as long as orthogonality (85−90°) of the subunits is retained upon charging.[17] Besides the well-investigated prototype **2**,[18-20] higher oligoanthrylenes ($m > 1$) have not previously been studied.

Herein, we report the synthesis of novel anthrylenes **3a**, **3b**, and **4** and the results of electron paramagnetic resonance/electron nuclear double resonance (EPR/ENDOR) spectroscopic studies of their corresponding radical anions prepared by chemical reduction. These studies yield new insight into the intramolecular electron transfer between anthracene moieties in the monocharged state, demonstrating a sensitive dependency on the alkyl substitution pattern of the compounds, introduced for solubility reasons, and the ion pair conditions.

Chart 2

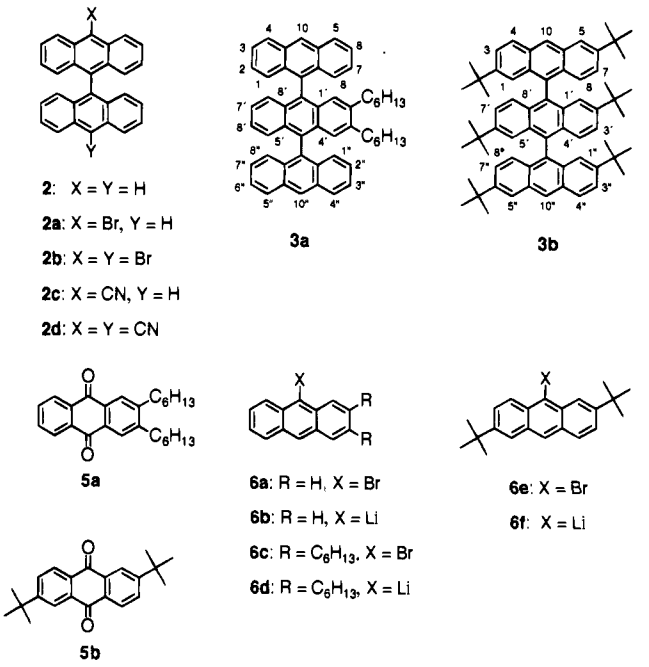

2: X = Y = H
2a: X = Br, Y = H
2b: X = Y = Br
2c: X = CN, Y = H
2d: X = Y = CN

3a **3b**

5a

6a: R = H, X = Br
6b: R = H, X = Li
6c: R = C_6H_{13}, X = Br
6d: R = C_6H_{13}, X = Li

6e: X = Br
6f: X = Li

5b

Upon further charging of the monoanions, higher spin states of the consecutively charged anthracene subunits in **2**, **3a**, and **4** and in a corresponding polymer sample have been obtained and are discussed in detail.

2. Results and Discussion

2.1. Synthesis. The parent compound **2** was prepared according to the literature.[21] The syntheses of **2a**, **2b**, **2c**, and **2d** (Chart 2) are largely based on know procedures.[22] Optimization of the reactions, however, required several modifications (see Experimental Section). Bromination of **2** afforded the bromo derivatives **2a** and **2b** and opened a simple route to the corresponding cyano derivatives. Thus, **2a** and **2b** can be converted with CuCN in relatively high yields to **2c** and **2d**.

The starting materials of the trimers **3a,b** are the anthraquinones **5a,b** (alkyl-substituted in the 2- and 3-positions or 2- and 6-positions), which can easily be prepared on a large scale by standard procedures.[23] Compounds **5a,b** react with the organolithium species **6b** and **6f**[24] to yield the coupling products **7a,b**, (Chart 3) which after treatment with hydrogen iodide/hypophosphorous acid provide the soluble trianthrylenes **3a** and **3b**.

The tetramer **4** is formed by reaction of 10,10′-bianthronylidene (**8**) with lithium compound **6d**,[24] followed by aromatization and chromatographic purification. In a similar fashion polymeric anthrylenes are formed by reaction of 10,10″-dilithio-9,10-trianthrylene with 10,10′-bianthronylidene.[24]

2.2. Monoradicals in Solution. Reduction of the anthrylenes with potassium in solution under high vacuum yields first blue-fluorescent and then green-colored solutions of the paramagnetic monoanions, which were characterized by UV/vis and EPR/ENDOR spectroscopy in the same sample tube. These parallel measurements have also been used to carefully control the reduction process.

(12) (a) Iwamura, H. *Adv. Phys. Org. Chem.* **1990**, *26*, 179. (b) Miller, J. S.; Epstein, A. J. *Angew. Chem., Int. Ed. Engl.* **1994**, *33*, 385. (c) Borden, W. T.; Iwamura, H.; Berson, J. A. *Acc. Chem. Res.* **1994**, *27*, 109. (d) Baumgarten, M.; Müllen, K. chapter 7 in *Top. Curr. Chem.* **1994**, *169*, 1. (e) Rajca, A. *Chem. Rev.* **1994**, *94*, 871. (f) Kurreck, H. *Angew. Chem.* **1993**, *105*, 1472.

(13) (a) Proceedings of the Symposium on Ferromagnetic and High Spin Molecular Based Materials, Dallas, April 1989. *Mol. Cryst. Liq. Cryst.* **1989**, 176. (b) Proceedings of the Symposium on Chemistry and Physics of Molecular Based Magnetic Materials. Iwamura, H.; Miller, J. S.; Eds.; *Mol. Cryst. Liq. Cryst.* **1993**, *232*, 1−360; 233, 1−366.

(14) (a) Veciana, J.; Vidal, J.; Jullian, N. *Mol. Cryst. Liq. Cryst.* **1989**, *176*, 443. (b) Kahn, O. *Struct. Bonding* **1987**, *68*, 89. (c) Kahn, O.; Pei, Y.; Journeaux, Y. *Mol. Cryst. Liq. Cryst.* **1989**, *176*, 429. (d) Dougherty, D. A. In *Research Frontiers in Magnetochemistry*; Connor, C. O., Ed.; World Scientific Publishing: River Edge, NJ, 1992.

(15) (a) Whangbo, M.-H. *Acc. Chem. Res.* **1983**, *16*, 95. (b) Salem, L.; Rowland, C. *Angew. Chem., Int. Ed. Engl.* **1972**, *11*, 91.

(16) (a) Baumgarten, M.; Müller, U.; Bohnen, A.; Müllen, K. *Angew. Chem., Int. Ed. Engl.* **1992**, *31*, 448. (b) Baumgarten, M.; Müller, U. *Synth. Met.* **1993**, *57*, 4755.

(17) (a) Müllen, K.; Baumgarten, M.; Tyutyulkov, N.; Karabunarliev, S. *Synth. Met.* **1991**, *40*, 127. (b) A ground state triplet of $2^{2\bullet-}$ is also predicted from semiempirical calculations (mopac 6) for AM1 (Stewart, J. J. P. *J. Comput. Chem.* **1989**, *2*, 209) optimized geomtries with OPEN(2,2), CI = 6, as used frequently by other authors, e.g., Lahti et al. also cited in ref 42d.

(18) Hoshino, H.; Kimamura, K.; Imamura, M. *Chem. Phys. Lett.* **1973**, *20*, 193.

(19) (a) Dietrich, M.; Mortensen, J.; Heinze, J. *Angew. Chem., Int. Ed. Engl.* **1985**, *24*, 508. (b) Mortensen, J.; Heinze, J. *J. Electroanal. Chem.* **1985**, *175*, 333. (c) Hammerich, O.; Saveant, J. M. *J. Chem. Soc., Chem. Commun.* **1979**, 938. (d) Mortenson, J.; Heinze, J.; Herbst, H.; Müllen, K. *J. Electroanal. Chem.* **1992**, *324*, 201. (e) Meehrholz, K.; Heinze, J. *J. Am. Chem. Soc.* **1990**, *112*, 5142.

(20) (a) Solodovnikov, S. P.; Zaks, Y. B. *Akad. Nauk. SSSR, Ser. Khim.* **1969**, *6*, 1375. (b) Solodovnikov, S. P.; Kabachnik, M. J. *J. Akad. Nauk. SSSR, Ser. Khim.* **1969**, *6*, 471. (c) Grampp, G.; Kapturkiewicz, A.; Salbeck, J. *Chem. Phys.* **1994**, *187*, 391.

(21) Bell, F.; Waring, D. H. *J. Chem. Soc.* **1949**, 267.

(22) Callas, R.; Lalande, R.; Ricordeau, F.; Delpine, M. *Compt. Rend.* **1961**, 136.

(23) Müller, U.; Enkelmann, V.; Adam, M.; Müllen, K. *Chem. Ber.* **1993**, *126*, 1217.

(24) Müller, U. Ph.D. Thesis, University of Mainz, Germany, 1993.

Chart 3

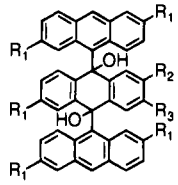

7a: $R_1 = H$, $R_2 = R_3 = C_6H_{13}$

7b: $R_1 = R_2 = C(CH_3)_3$, $R_3 = H$

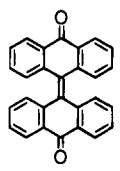

8

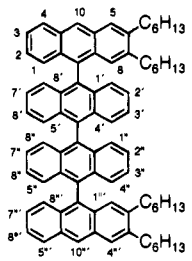

4

Table 1. Hyperfine Coupling Constants (mT) of the Monoradicals 2^+, 2^-, $2c^-$, $2d^-$, $3a^-$, $3b^-$, and 4^-

	1, 4, 5, 8[a]	2, 3, 6, 7[a]	9, 10[a]
2^-/loc[b]	0.264 (4 H)	0.144 (4 H)	0.574 (1 H)
2^-/deloc[b]	0.133 (8 H)	0.064 (4 H)	0.281 (2 H)
		0.087 (4 H)	
2^+/deloc[c]	0.140 (8 H)	0.062 (8 H)	0.350 (2 H)
$2c^-$/loc[b,d]	0.262 (2 H)	0.108 (2 H)	
	0.233 (2 H)	0.045 (2 H)	
$2d^-$/deloc[b]	0.111 (4 H)	0.060 (4 H)	
	0.100 (4 H)	0.034 (4 H)	
$3a^-$/loc[b]	0.286 (2 H)	0.165 (2 H)	0.531 (1 H)
	0.266 (2 H)	0.136 (2 H)	
$3b^-$/loc[b]	0.286 (2 H)	0.166 (2 H)	
	0.243 (2 H)		
4^-/loc[b]	0.264 (4 H)	0.144 (4 H)	
4^-/deloc[b]	0.135 (8 H)	0.075 (8 H)	

[a] Number of π-centers. [b] K^+ as counterion and THF as solvent (T = 200–250 K). [c] $SbCl_5$ as oxidant and CH_2Cl_2 as solvent (T = 250 K). [d] ^{14}N hfc = 0.083 mT.

The identification of the different monoanionic radical species rests upon analyses of the EPR and ENDOR spectra, e.g., on the number of multiplicity of the hyperfine coupling constants.[25] Formation of the dianions has thoroughly been excluded by UV/vis control and low-temperature EPR measurements, where biradicals should be envisaged. The results of this analysis are summarized in Table 1 together with the hyperfine coupling constants of the paramagnetic cation of **2**, which was generated in methylene chloride upon addition of antimony pentachloride ($SbCl_5$). The assignment of the hyperfine coupling constants given in Table 1 is based on comparison with spin density distributions in the radical anion and cation of anthracene, respectively, where the sequence of local spin densities is $\varrho(9,10) \gg \varrho(1,4,5,8) > \varrho(2,3,6,7)$.

The central question to deal with is whether the unpaired electrons of oligoanthrylene monoanions are localized in one electrophoric subunit or undergo a rapid hopping between two or more subunits, leading to an effective delocalization of the spin density within the time scale of the EPR experiment, and how different substitution patterns affect the electron-hopping rate constant.

The following criteria can be applied: (1) In the radical anions with the unpaired electron localized on one anthracene moiety, the magnitudes of related proton hyperfine coupling constants resemble those of anthracene or substituted anthracene radical anions, a(H-9,10) = 0.5–0.6 mT, a(H-1,4,5,8) = 0.2–0.3 mT, a(H-2,3,6,7) = 0.1–0.2 mT.[26,27] (2) Localization of the unpaired electron within one anthracene subunit lowers the symmetry of the system. This symmetry deformation can be investigated by simply counting the number of equivalent protons giving rise to a particular coupling constant. (3) Radical anions with their unpaired electron symmetrically delocalized over two subunits in a biselectrophoric system possess hyperfine coupling constants half as large as those in anthracene radical anions with twice the number of hyperfine coupled nuclei.

That one is still dealing with an electron-hopping process and not with extended conjugation results from measurements of the optical absorption spectra which possess a much faster time scale (10^{-11} s). The absorption spectra do not show a characteristic bathochromic shift, neither for the neutral nor for the monocharged species, which is evidence for independent chromophores. Relying on these experimental criteria, the monoanions of the synthesized oligoanthrylenes were investigated.

In the case of $2^{\bullet-}/K^+$/THF a superposition of two species can be detected for the partially monoreduced state, which is still in equilibrium with some neutral compound. One species has large hyperfine couplings (hfcs) comparable to those of the monoradical of anthracene,[26] and one species shows just twice the number of hyperfine splittings in the EPR spectra (Table 1). No change in relative intensities nor line widths of the alternant EPR signals are observed upon variation of the temperature and dilution of the sample. This is in agreement with earlier work on $2^{\bullet-}$ where also no temperature effect could be measured in solution even when using large ammonium salts as counterions.[20] The relative intensities of the two sets of EPR lines, on the other hand, sensitively depend on the stage of reduction, i.e., the amount of charged species in solution. At very low radical concentrations generated upon mixing of the solution of **2** with a solution of solvated electrons from contacting THF on potassium, an EPR spectrum with half the hfcs of the anthracene monoanion is observed, and thus, a complete delocalization of the unpaired electron over the two anthracene subunits is determined by ENDOR. It can be concluded that the electron spin exchange over two identical anthracene moieties is fast on the EPR time scale under the prevailing experimental conditions.

The UV/vis spectra of this sample indicate the coexistence of neutral and monocharged species for which the maximum absorption bands occur at wavelengths of 680 and 720 nm, respectively, comparable to that for the monoanion of anthracene (680, 709 nm) (Table 2). Consequently, the intramolecular electron transfer is slow on the time scale of optical absorption spectroscopy ($<10^{-11}$ s).

With increasing monoradical concentration of $2^{\bullet-}/K^+$, only a change in relative intensities of the longest wavelength transition can be detected in the optical spectra, while at this stage of reduction the EPR spectra change to spectra with alternating line widths as mentioned above. The experimental spectrum can be described as a superposition of EPR signals of an effectively delocalized species and a localized species, leading to an alternant line width pattern (Figure 1A). The experimental EPR spectra in this intermediate case can be

(25) (a) Kurreck, H.; Kirste, B.; Lubitz, W. *Angew. Chem., Int. Ed. Engl.* **1984**, *24*, 173. (b) Kurreck, H.; Kirste, B.; Lubitz, W. In *Electron Nuclear Double Resonance Spectroscopy of Radicals in Solution*; Marchand, A.p., Ed.; VCH: Weinheim, Germany, New York, 1988.

(26) Tuttle, R. *J. Am. Chem. Soc.* **1962**, *84*, 2839.

(27) (b) Bolton, J. R. *J. Chem. Phys.* **1964**, *40*, 3307. (b) Bauld, N. L.; McDermed, J. D.; Hudson, C. E.; Reim, Y. S.; Zoeller, J.; Gordon, R. D.; Hyde, J. S. *J. Am. Chem. Soc.* **1969**, *91*, 6666.

Table 2. λ_{max} Values (nm) from Optical Absorption Spectra of Anthrylenes **2**, **2c**, **2d**, **3a**, **3b**, and **4** and Corresponding Reduction Products[a]

	anthracene	**2**	**2c**	**2d**	**3a**	**3b**	**4**
neutral	377	391	413	414	403	402	406
monoanion[b]	709	669			671		682
dianion[b]	625	735					
trianion[b]		463					
tetraanion[b]		629					

[a] All spectra measured in THF solution (T = 293 K). [b] K^+ as counterion.

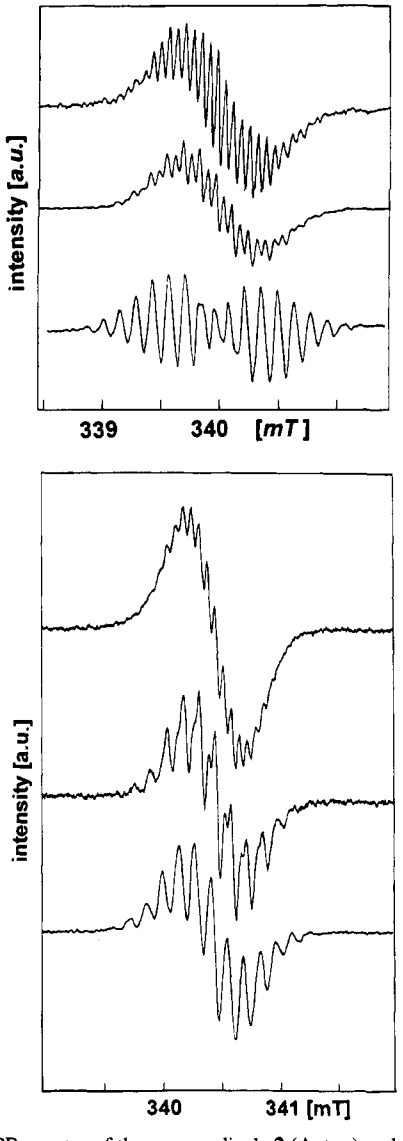

Figure 1. EPR spectra of the monoradicals **2** (A, top) and **4** (B, bottom) in THF solution (counterion K^+; T = 270 K) with increasing reduction process, i.e., radical (respectively counterion) concentration.

computer simulated perfectly, by adding the simulations for the localized and delocalized states with the hfcs and multiplicities given in Table 1. Upon further charging of neutral molecules, the spin delocalized form disappears and only a spin localized form can be detected in the EPR/ENDOR spectra. It seems that with increasing monoradical (respectively counterion) concentrations the polarity of the solutions is changed, thereby controlling the electron self-exchange. This change in spin distribution upon the reduction process is similar to findings made by Gerson et al.[28] on other biselectrophores.

In the case of the radical cation of **2** generated by $SbCl_5$ in methylene chloride a complete spin delocalization is observed by nearly twice the number of hyperfine splittings in the EPR and half the size of hfcs in the ENDOR spectrum compared to those of the radical cation of anthracene.[26] The EPR intensity is much larger than in the corresponding anion, leading us to assume that even higher radical concentrations are needed before localization takes place. One can thus deduce that under these experimental conditions solvent-separated ion pairs (SSIP) dominate, enabling a fast electron exchange between the subunits.

Substitution of one anthracene moiety of **2** in the 10-position with a cyano group leads to 10-monocyano-9,9′-bianthryl (2c). Due to the strong acceptor behavior of the cyano group, only spin localization in the substituted anthracene ring of **2c**$^{\bullet-}$/K^+/THF is detectable by EPR/ENDOR, even in the weakly reduced state. Hfcs corresponding to the coupling of the electron spin with the nitrogen atom are small and were not found in the ENDOR spectrum. They should appear in the very low frequency range. Therefore, the computer simulation of the EPR spectrum is only in accordance with the experimental spectrum of **2c**$^{\bullet-}$ by consideration of a ^{14}N hfc of 0.083 mT. As determined by cyclovoltammetric studies, a remarkable difference between the first reduction steps of dimers **2** and **2c** appears (**2**, $E^1_{1/2}$ = −2.17 V; **2c**, $E^1_{1/2}$ = −1.60 V; vs ferrocene calibration, $TBAPF_6$, THF, T = 293 K, ν = 100 mV/s) due to the strong electron-withdrawing conjugative influence of the cyano group. Thus, the cyano-substituted anthracene unit in **2c** possesses a distinctly higher affinity for the negative charge than the unsubstituted one, and the degeneracy of an intramolecular hopping process in **2c**$^{\bullet-}$/K^+ is removed by the different redox potentials of the subunits. Consequently, the unsymmetrical cyano substitution implies spin localization within the time scale of the EPR experiment.

When going to the radical anion of 10,10′-dicyano-9,9′-bianthryl (**2d**), the situation of charge distribution changes drastically. In this case with two identical substituted anthracene moieties only a spin delocalized species can be detected with much smaller ^1H hfcs.

For the radical anion of trimer **3a** only charge localized states are detected in the case of **3a**$^{\bullet-}$/K^+/THF and **3a**$^{\bullet-}$/K^+/MTHF even at variable temperature ranges from 220−300 K. The hyperfine coupling constants of the ring protons of the described monoanions are very similar to those of the monomeric reference system, the anthracene radical anion. A reduced symmetry is indicated by the nonequivalence of the 1,4-protons (0.286, 0.266 mT) and 2,3-protons (0.165, 0.136 mT) in highly resolved ENDOR spectra. In addition, a large hfc constant corresponding to the proton in the 10-position can be observed. These findings are only consistent with a localization of the electron spin on a terminal anthracene residue of **3a**$^{\bullet-}$/K^+ without solubilizing alkyl groups. The charging of the central electrophoric unit occurs at higher potential due to the electron-donating effect of the alkyl groups. Here, spoken in terms of the Marcus theory,[29,30] the ground state energy difference $\Delta G°$ between the two potential minima is no longer zero, and increases the activation barrier for the intramolecular electron transfer. This small potential change leads to charge localization in **3a**$^{\bullet-}$/K^+ already at room temperature as in the case of **2c**$^{\bullet-}$/K^+.

The mode of spin density distribution changes for the radical anion of trimer **3b**, where each anthracene unit is substituted

(28) (a) Gerson, F.; Huber, W.; Martin, W. B.; Caluwe, P.; Pepper, T.; Szwarc, M. *Helv. Chim. Acta* **1984**, *67*, 416. (b) Gerson, F.; Wellauer, T.; Oliver, A. M.; Paddon-Row, M. N. *Helv. Chim. Acta* **1990**, *73*, 1586.

(29) (a) Marcus, R. A. *J. Chem. Phys.* **1956**, *24*, 979. (b) Marcus, R. A. *J. Phys. Chem.* **1963**, *67*, 853, 2884. (c) Marcus, R. A. *J. Chem. Phys.* **1965**, *43*, 679.

(30) (a) Hush, N. S. *Trans. Faraday Soc.* **1961**, *57*, 557. (b) Hush, N. S. *Chem. Phys.* **1975**, *10*, 361.

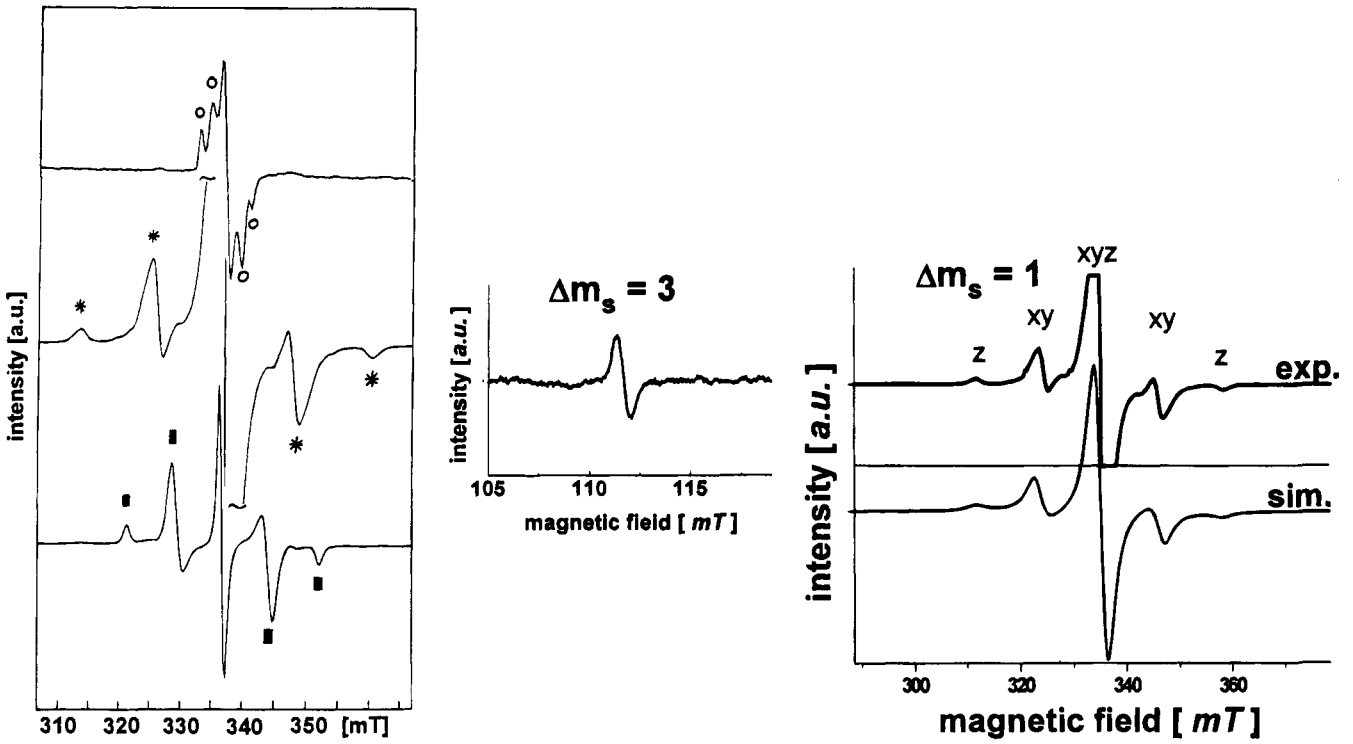

Figure 2. (A, left) EPR spectra of **3a** upon reduction (MTHF, K^+, 150 K). In each case the largest spin state splitting is labeled: (O) diradical (small D, $S = 1$, $\mathbf{3a}^{2\bullet-}$); (★) triradical ($S = 3/2$, $\mathbf{3a}^{3\bullet-}$); (■) diradical (large D, $S = 1$, $\mathbf{3a}^{4-}$). (B, middle and right) Experimental and computer simulated EPR spectra of $\mathbf{3a}^{3\bullet-}$ together with the $|\Delta m_s| = 3$ transition at $H_{res}/3$ ($T = 40$ K).

with solubilizing *tert*-butyl groups in the 2- and 6-positions. Due to the missing proton hyperfine coupling for the 10-position and the appearance of three hfcs with values similar to the 1-, 3-, and 4-positions of $\mathbf{3a}^{\bullet-}/K^+$, one can deduce spin localization in the central anthracene perimeter of $\mathbf{3b}^{\bullet-}/K^+$. Thus, the different substitution pattern between **3a** and **3b** demonstrates a "fine tuning effect" of spin localization in monocharged multielectrophoric anthrylene systems caused by different alkyl substitution patterns.

In the weakly reduced state of tetraanthrylene **4**, a situation similar to the one for $\mathbf{2}^{\bullet-}/K^+$ occurs. In the very beginning of the reduction the experimental EPR spectrum is comparable to $\mathbf{2}^{\bullet-}_{del}$ but extends over a smaller total width. From the computer simulation it is well evidenced that no protons from positions 9 and 10 with the largest MO coefficient contribute to this spectrum. Thus, first an electron delocalization over the two central anthracene units is observed, while slightly further reduction leads to a mixture of localized and delocalized species in the intermediate state evidenced by alternating line widths and intensities in the EPR spectra (Figure 1B). At even higher radical and counterion concentrations the unpaired electron is localized on one central anthracene unit. The EPR/ENDOR investigations of $\mathbf{4}^{\bullet-}/K^+$ evidence the pure intramolecular process by the much smaller total width of the EPR/ENDOR spectra due to the missing protons in positions 9 and 10, and nicely summarizes two factors determining spin localization and effective delocalization of the studied 9,10-anthrylenes.

(i) In the case of anthracene moieties with different alkyl substitution patterns the electron transfer can no longer be regarded as degenerate, due to the different potentials of the subunits caused by electronic effects of the substituents. An energetic difference, $\Delta G°$, between the potential minima of the subunits contributes to the total activation energy $\Delta G^{\ddagger}$ and decreases the intramolecular electron transfer rate in 9,10-anthrylenes. Consequentely, the electron transfer between differently substituted subunits cannot be detected under the experimental conditions for EPR/ENDOR spectroscopy. It is, thus, possible to control the energy profile of an electron-hopping process in oligo(9,10-anthrylene)s by choosing an appropriate mode of substitution of single anthracene electrophores.

(ii) The electron transfer rate between two identical anthracene electrophores (degenerate electron transfer) in $\mathbf{2}^{\bullet-}$, $\mathbf{2d}^{\bullet-}$, and $\mathbf{4}^{\bullet-}$ is influenced by the radical and counterion concentration, which allows a switching between effectively delocalized and localized states within the time scale of the EPR experiments. This can be attributed to the fact that the electron transfer must be accompanied by a migration of the counterion and, thus, by a reorganization of the ion pair structure and the solvent shell. The energy involved contributes to the total reorganization energy λ_s.[29,30] Accordingly, the intramolecular electron exchange becomes slow at higher radical concentrations, enhancing the polarity of the solution, i.e., the rate constant is slowed below 10^{-7} s.

A comparison of the electronic absorption spectra of the monoanions of **2**, **3a**, and **4** demonstrates that in each case one anthracene unit is charged: the respective λ_{max} values (Table 2) are nearly independent of the number of repeating units and reveal the anthracene units to exist as independent electrophores in monocharged states of molecules. A small bathochromic shift of the longest wavelength band with increasing chain size can be detected, but his may also be caused by the different substitution patterns.

2.3. High-Spin States. Further reduction of the monoanions ($\mathbf{2}^{\bullet-}/K^+$, $\mathbf{3a}^{\bullet-}/K^+$, and $\mathbf{4}^{\bullet-}/K^+$) with potassium leads to triplet states of the dianions or to higher spin multiplicities in the more highly charged derivatives. The EPR spectra of randomly oriented radicals in frozen glass (Figures 2 and 3) result from the magnetic dipole interactions among unpaired electrons, not from the anisotropy of the **g** value or the hyperfine coupling tensor. Since the orbital angular momentum is generally quenched in organic homonuclear conjugated radicals,[31] the **g**

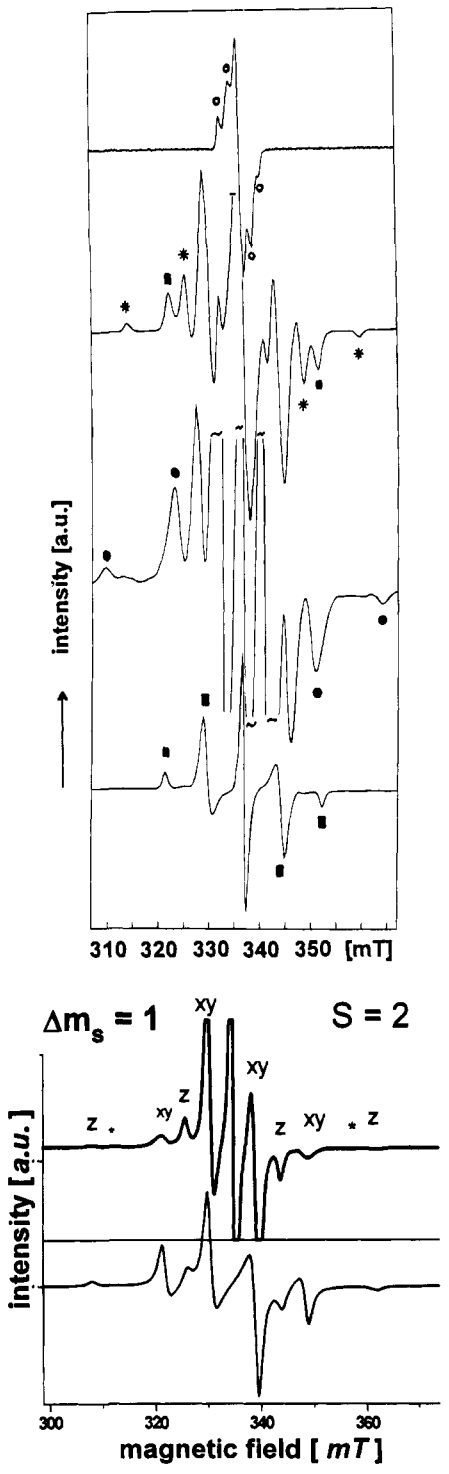

Figure 3. (A, top) EPR spectra of **4** upon reduction. The different spin states are labeled: (○) diradical (small D, $S = 1$, $\mathbf{4a}^{2\bullet-}$), (★) triradical ($S = 3/2$, $\mathbf{4a}^{3\bullet-}$), (●) tetraradical ($S = 2$, $\mathbf{4a}^{4\bullet-}$), (■) diradical (large D, $S = 1$). The lowest spectrum cannot be assigned to a defined redox state: $\mathbf{4}^{5-}$ or $\mathbf{4}^{6-}$. It shows the interaction between two unpaired electrons on adjacent anthracene units. (B, bottom) Experimental and computer simulated EPR spectra of $\mathbf{4a}^{4\bullet-}$. The asterisk labels a small amount of $S = 3/2$ contribution also giving rise to the central line.

tensor is nearly isotropic. Let us consider the theoretical predictions for molecules with electron spin $S > 1/2$.[32] In the case of small hyperfine coupling (electron spin−nuclear spin) compared to the electron spin−electron spin interaction ($S\cdot\mathbf{A}\cdot I \ll S\cdot\mathbf{D}\cdot S$) the spin Hamiltonian consists of the Zeemann and the fine structure term as given by eqs 1 and 2,where β is the

$$H = \beta\mathbf{H}\mathbf{G}\cdot S + S\cdot\mathbf{D}\cdot S \quad (1)$$

$$H = \beta\mathbf{H}\mathbf{g}S + D[S_z^2 - (1/3)S(S+1)] + E(S_x^2 - S_y^2) \quad (2)$$

Bohr magneton, **H** is the applied magnetic field, and D and E are the zero-field splitting (zfs) parameters. Thus, the zero-field tensor **D** is traceless and thereby described usually only by the two parameters D and E which can be taken from the observed EPR spectra. E is the asymmetry parameter and zero for a linear radical and for molecules with a trigonal axis of symmetry.

The EPR spectra of the highly charged species of **2**, **3a**, and **4** in frozen solution reveal a characteristic zero-field splitting indicating high-spin alignment. Corresponding D values are presented in Table 3, which are discussed in detail.

Treatment of a THF solution of $\mathbf{2}^{\bullet-}/K^+$ with a potassium mirror produces $\mathbf{2}^{2\bullet-}/K^+$. The well-resolved $|\Delta m_s| = 1$ region of the EPR spectrum at 150 K consists of four symmetrically placed resonances (corresponding to H_{z1}, H_{xy1}, H_{xy2}, and H_{z2}), which can be assigned to a triplet species with axial symmetry ($E = 0$). The characteristic zero-field splitting constant D was determined to be 16.5 mT from the difference of the H_{z1} and H_{z2} transitions.[33] Assuming the point dipole approximation in the expression of D ($D = 3g^2\beta^2/4r^3$),[34] the splitting corresponds to an average distance of $R = 0.55$ nm between the two interacting spins. This finding is in excellent agreement with previously reported results of $\mathbf{2}^{2\bullet-}/2Na^+$ generated under different experimental conditions,[18] and indicates that each electrophoric subunit of **2** is charged. Furthermore, the axial symmetry reflected in the received spectrum is in accordance with an almost orthogonal arrangement of the anthracene moieties. The $|\Delta m_s| = 2$ transition observed at half resonance field gives additional evidence that the detected species is unambiguously in a triplet state.

Successive reduction of $\mathbf{3a}^{\bullet-}/K^+$ on a potassium mirror first yields a biradical with an EPR spectrum containing four symmetric absorptions in the axial resonance field, which is typical for a triplet species with vanishing E value. The zfs constant D is 3.9 mT, corresponding to an average distance of $R = 0.89$ nm as estimated by the point dipole approach. According to the EPR results of the monoradical and additional cyclovoltammetric measurements of **3a**,[16a] the splitting clearly points to a charging of the two terminal electrophores which are charged at slightly lower potential than the alkyl-substituted central unit. Interestingly, the formally forbidden "half-field" $|\Delta m_s| = 2$ transition cannot be observed in the spectrum of $\mathbf{3a}^{2\bullet-}/2K^+$. Due to the EPR selection rules for zfs, only a large zfs leads to a great intensity of the $|\Delta m_s| = 2$ transition.[31] Thus,

Table 3. Zero-Field Splitting Parameters Observed for the Charged Derivatives of **2**, **3a**, and **4** in Glassy Solutions of MTHF ($T = 150$ K, K^+ as Counterion) and Corresponding Average Distances R of Interacting Spins Estimated by Using the Point Dipole Approach[34]

	$\mathbf{2}^{2-}$ [a]	$\mathbf{3a}^{2-}$	$\mathbf{3a}^{3-}$	$\mathbf{3a}^{4-}$	$\mathbf{4}^{2-}$	$\mathbf{4}^{3-}$	$\mathbf{4}^{4-}$	$\mathbf{4}^{5-}$ or $\mathbf{4}^{6-}$
D (mT)	16.5	3.85	11.5	15.2	3.6	11.4	8.9	14.5
R (nm)	0.55	0.89			0.92			

[a] THF as solvent.

(31) Slichter, C. P. *Principles of Magnetic Resonance*; Harper & Row: New York, 1963; Chapters 4 and 7.
(32) Weltner, W. *Magnetic Atoms and Molecules*; Van Nostrand Reinhold: New York, 1983; Chapter 5.
(33) Wasserman, E.; Snyder, L. C.; Yager, W. A. *J. Chem. Phys.* **1964**, *41*, 1763.
(34) Carrington, A.; McLachlan, A. D. *Introduction to Magnetic Resonance*; Harper & Row: New York, 1967; p 130.

in spite of the small D value of $\mathbf{3a}^{2\bullet-}/2K^+$, the half-field absorption should be extremely weak and might not be detected.

Successive reduction of the dianion of **3a** affords an EPR signal, which must be assigned to a quartet state of $\mathbf{3a}^{3\bullet-}/3K^+$ (Figure 2), in which each anthracene subunit is charged. In the usual case of $D \ll g\beta\mathbf{H}$, EPR selection rules allow five $|\Delta m_s| = 1$ lines (corresponding to H_{z1}, H_{xy1}, H_{xyz1}, H_{xy2}, and H_{z2} transitions) in randomly oriented samples of axial symmetric quartet molecules. Then, the total spectral width is $4D$ (distance between H_{z1} and H_{z2} lines) with the H_{xy1} and H_{xy2} transitions placed at a distance of $2D$ and simultanuous increase of a central H_{xyz1} line.[35] Indeed, all the theoretically predicted features for an uniaxial ($E = 0$) quartet molecule are represented in the obtained EPR spectrum of $\mathbf{3a}^{3\bullet-}/3K^+$ (Figure 2). The corresponding D value was determined to be 11.5 mT and is supported by computer simulation of the experimental EPR spectrum.[36] In addition, an intense $|\Delta m_s| = 2$ transition was detected at half-field. The $|\Delta m_s| = 3$ transition associated with a three-electron flip, however, could not be observed at this temperature (130 K). Since the forbidden Δm_s transitions are often used for unambiguous definition of higher spin states, we put a large effort into the detection of the $|\Delta m_s| = 3$ transition, and when applying liquid helium as coolant to profit from signal enhancement at low temperatures, we were able to measure the $|\Delta m_s| = 3$ transition, leaving no doubt of the $S = 3/2$ state.[37,38]

Finally, upon further reduction of $\mathbf{3}^{\bullet-}/3K^+$ an EPR spectrum appears containing four symmetrical lines in the resonance field and a $|\Delta m_s| = 2$ transition at half-field, corresponding to an axial symmetric diradical of the tetraanion of **3a**. The D value of 15.2 mT, comparable to that of $\mathbf{2}^{2\bullet-}/2K^+$, points toward a diradical where two neighboring units carry a spin. In summary, the EPR frozen spectra of the reduction sequence of **3a** with assignment to the redox states are presented in Figure 2.

Anologously to $\mathbf{3a}^{\bullet-}/K^+$, stepwise reduction of $\mathbf{4}^{\bullet-}/K^+$ affords EPR signals in frozen solution, which confirm the initial formation of a biradical of the dianion $\mathbf{4}^{2\bullet-}/2K^+$. Here again, the splitting of the $|\Delta m_s| = 1$ region ($D = 3.8$ mT, $E = 0$) points toward an axial symmetric triplet species, in which the charges are located on distant anthracenes. The small difference in D ($\Delta D = 0.1$ mT) compared to the zfs in $\mathbf{3a}^{2\bullet-}/2K^+$ does not allow differentiation between charge localization on each terminal electrophore and a charge localization on two anthracenes spaced by just one anthrylene unit as in $\mathbf{3a}^{2\bullet-}/2K^+$. In view of the slightly higher reduction potential of an alkyl-substituted anthracene and the charge localization in a central anthracene unit for the monoradical, the latter situation should be favored and can be explained by the Coulombic repulsion of the two charges on the same molecule. As in the case of

Chart 4

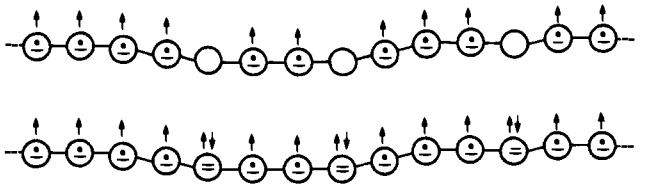

$\mathbf{3a}^{2\bullet-}/2K^+$, no half-field transition can be observed for $\mathbf{4}^{2\bullet-}/2K^+$, due to the small zfs; i.e., small interaction of unpaired spins.

By further reduction $\mathbf{4}^{2\bullet-}/2K^+$ is transformed into the trianion of **4**, which similar to $\mathbf{3a}^{3\bullet-}/3K^+$ shows an EPR spectrum with typical splitting pattern of an uniaxial quartet state (Figure 3), as discussed above. The measured D value of 11.4 mT is also similar to that of $\mathbf{3a}^{3\bullet-}/3K^+$.

Additional reduction of $\mathbf{4a}^{3\bullet-}/3K^+$ with potassium leads to even larger fine tensor components in the frozen solution EPR spectrum, which finally exceed the former $S = 3/2$ state components (Figure 3) and must be assigned to a quintet state ($S = 2$) of $\mathbf{4}^{4\bullet-}/4K^+$ ($D = 8.9$ mT; $E = 0$). According to theoretical predictions, a randomly oriented sample of a uniaxial quintet gives rise to a total spectral width of $6D$ (distance between the outermost H_z lines) with the additional appearance of H_{xy} and H_z absorptions at distances of $3D$ and $2D$, respectively. Furthermore, as investigated by Wassermann et al.,[38d] the absolute D values of comparable spin systems become smaller as S increases. The excellent agreement of theoretical predictions and experimental findings for the measured spectrum establishes the quintet state of $\mathbf{4}^{4\bullet-}/4K^+$. Again, a relative intense $|\Delta m_s| = 2$ absorption at half-field and a much weaker $|\Delta m_s| = 3$ transition (only detectable at even lower temperatures, $T =$ ca. 40 K), typical for systems in a multiplet state, are also observed. The EPR fine structure, however, points to the coexistence of a small amount of the triplet of $\mathbf{4}^{3-}/3K^+$ whereby the relative signal intensities of both species depend sensitively on the sample preparation. The different line patterns of the $S = 3/2$ and $S = 2$ states together with the shift from one spin state to the other upon reduction and the computer simulation leave no doubt about the spin states.

Finally, upon further reduction a triplet of an even more highly charged derivative of **4** ($\mathbf{4}^{5-}$ or $\mathbf{4}^{6-}$) can exclusively be detected by EPR (Figure 3). In accordance with the D values measured for $\mathbf{2}^{2\bullet-}/2K^+$ and $\mathbf{3a}^{4-}/4K^+$, the splitting in the resonance field of the final EPR spectrum ($D = 14.5$ mT) corresponds to an interaction of unpaired electrons located on neighboring anthracene units. For an overview, the EPR spectra measured during the reduction sequence of **4** are presented in Figure 3, while all measured D values and estimated R values are summarized in Table 3.

Following a further extension toward high-spin materials, we also reduced a soluble polymer sample ($n =$ ca. 20) where the low molecular weight fraction had been separated off by gel permeation chromatography. The polymer could successively be charged to a polyradical containing $S = 1$, $S = 3/2$, and even $S = 2$ states, with the same zero-field splitting as observed for the defined oligomers. In this sample nearly every repeating unit carries a spin. Since upon further charging the polymer sample was no longer soluble and precipitated from solution, it was not possible to find out whether higher spin states are excluded by interruption of spin coupling through an uncharged

(35) Brickmann, J.; Kothe, G. *J. Chem. Phys.* **1973**, *59*, 2807.

(36) We are grateful to Dr. Stoyan Karabunarliev who has written the computer program for simulation of the EPR spectra of arbitrary spin states ($S = 1-5.5$) by direct diagonalization of the spin Hamiltonian $H = g\mu_b\mathbf{H}\cdot\mathbf{S} + \mathbf{S}\cdot\mathbf{D}\cdot\mathbf{S}$. The program has been tested on examples by Ling, C. et al. (*J. Am. Chem. Soc.* **1992**, *114*, 9959) and Matsushita et al. (*J. Am. Chem. Soc.* **1992**, *114*, 7470).

(37) We wish to thank one reviewer who asked about this identification of $S = 3/2$, although it is not yet often been done since the intensities of the three transitions $|\Delta m_s| = 1$, 2, and 3 are expected in the ratio $1:(D/\mathbf{H})^2:(D/\mathbf{H})^4$.[38] In the anionic triradical of **3a**, the intensity of the $|\Delta m_s| = 3$ transition is about 10^{-8} relative to that of the $|\Delta m_s| = 1$ transition. This led to only two experimental proofs of the $|\Delta m_s| = 3$ transition so far in the literature.[38,39]

(38) (a) Weissman, S. I.; Kothe, G. *J. Am. Chem. Soc.* **1975**, *97*, 2538. (b) Weissmann, S. I. *J. Am. Chem. Soc.* **1975**, *97*, 2537. (c) Novak, C.; Kothe, G.; Zimmermann, H. *Ber. Bunsen-Ges. Phys. Chem.* **1974**, *78*, 265. (d) Wasserman, E.; Murray, R. W.; Yager, W. A.; Trozzolo, A. M.; Smolinsky, G. *J. Am. Chem. Soc.* **1967**, *89*, 5076.

(39) (a) Rajca, A.; Utamapanya, S. *J. Am. Chem. Soc.* **1993**, *115*, 2396. (b) Utamapanya, S.; Kakegawa, H.; Bryant, L.; Rajca, A. *Chem. Mater.* **1993**, *5*, 1053. (c) Rajca, A.; Rajca, S., Desai, S. *J. Am. Chem. Soc.* **1995**, *117*, 806.

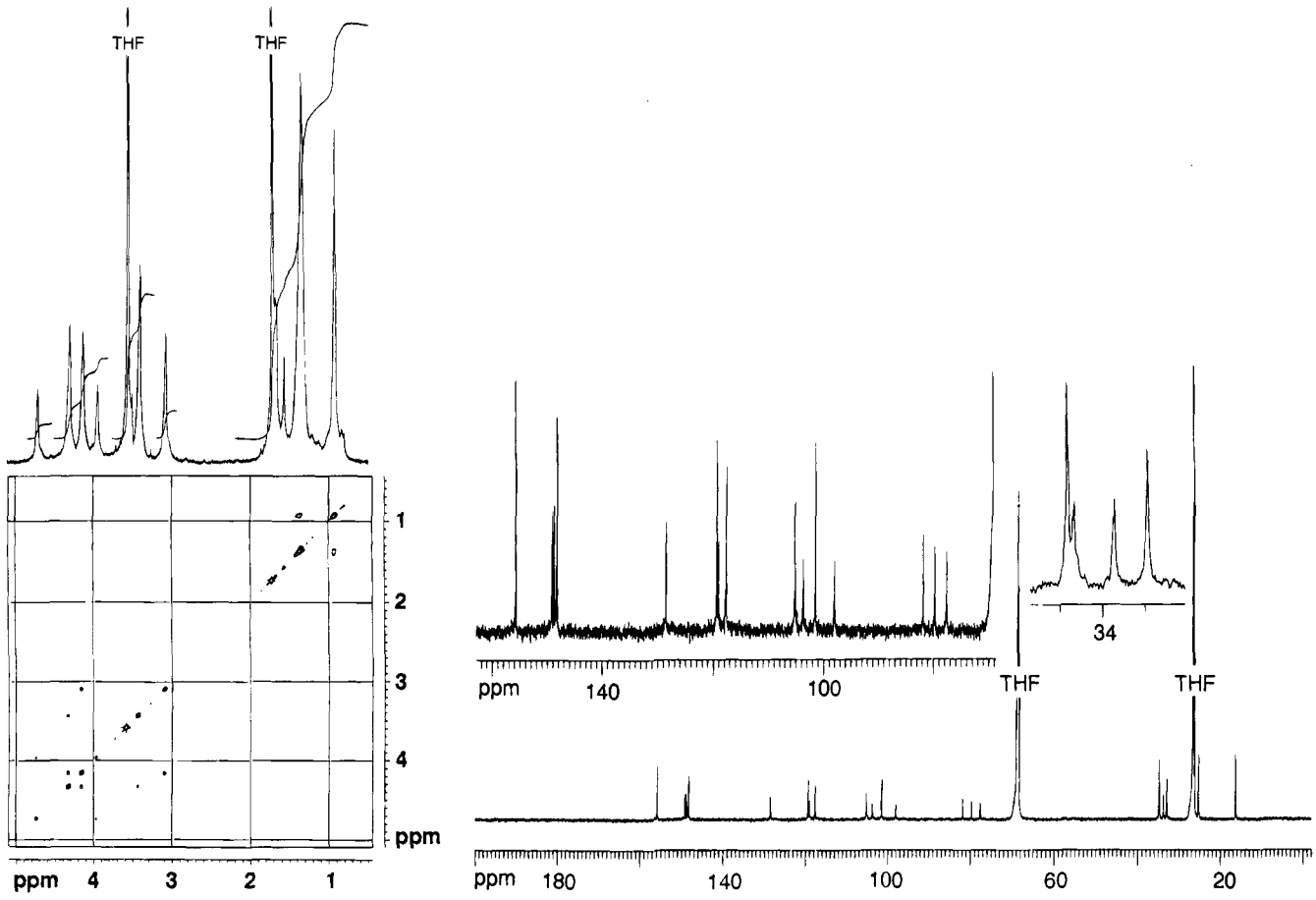

Figure 4. Partial NMR spectra for hexaanion $\mathbf{3a}^{6-}/6Li^+$ in THF-d_8 at 250 K: (A, left) ^1H NMR; (B, right) ^{13}C NMR (assignments to NMR signals are given in the Experimental Section).

or a doubly charged anthracene in between (Chart 4). As described by Iwamura[12a] for polycarbenes and very recently for poly(arylmethane) radicals,[12e,39] any nonmagnetic repeat unit will interrupt the total spin coupling, leaving separated high-spin parts.

2.4. NMR Investigations. The redox stability of the highly charged states is also proven by ^1H and ^{13}C NMR spectroscopy of the completely reduced blue diamagnetic $\mathbf{3a}^{6-}/Li^+/THF\text{-}d_8$. The analysis of the NMR data is straightforward, and we will only comment on its relation to the totally intact framework and the molecular geometry for the hexaanion of **3a** (for detailed spectroscopic data see the Experimental Section).

All the proton signals in the well-resolved ^1H NMR spectra (Figure 4) can be assigned with the aid of a H,H correlated 2D spectrum. Remarkably, the signals of the protons of $\mathbf{3a}^{6-}/Li^+$ are strongly shifted to high field in accordance with those for $\mathbf{2}^{4-}/Li^+/THF\text{-}d_8$.[40] This shift can be explained on the basis of π-charge densities resulting from simple MO models and of anisotropic paramagnetic ring current effects caused by doubly-charged neighboring anthracene rings.[41] Furthermore, the splitting patterns and relative intensities of the ^1H NMR signals substantiate without doubt the existence of an intact trianthrylene framework in $\mathbf{3a}^{6-}/6Li^+$. The number of resonances in the ^1H and ^{13}C NMR spectra (especially clarified by a ^{13}C spin-echo experiment) demonstrates a C_{2v} structure similar to the neutral compound on the time scale of the NMR experiments (10^{-5}–10^{-7} s). This finding points toward an orthogonal arrangement of the anthracene units in $\mathbf{3a}^{6-}/Li^+$.

(40) Huber, W.; Müllen, K. *J. Chem. Soc., Chem. Commun.* **1980**, 698.
(41) (a) Bock, B.; Kuhr, M.; Musso, H. *Chem. Ber.* **1976**, *109*, 1184. (b) Müllen, K.; Meul, T.; Schade, P.; Schmickler, H.; Vogel, E. *J. Am. Chem. Soc.* **1987**, *104*, 4992.

For a subsequent quenching reaction of $\mathbf{3a}^{6-}/Li^+$, the tubes were opened under argon and the solution was treated with dimethyl sulfate. The number of electrophilic reagents incorporated into the charged substrate, detectable by FD mass spectroscopy, provides independent evidence for the number of extra electrons in the ionic state.

Reduction of **4** for two weeks at 250 K with lithium metal also provides a deep blue solution of a diamagnetic species with chemical shifts of the ^1H NMR signals similar to those of $\mathbf{3a}^{6-}/6Li^+$, carefully assigned to $\mathbf{4}^{8-}/8Li^+$. A detailed NMR spectroscopic investigation, however, was inhibited by the sparing solubility of this species in THF-d_8.

2.5. Temperature Dependent Measurements. EPR measurements at different temperatures provide further insight into the stability and temperature dependence of the high-spin states of oligo(9,10-anthrylene)s and confirm their ground state spin multiplicity.

"Curie law" studies of triplet species by EPR spectroscopy are normaly based on the temperature dependence of the intensity of the $|\Delta m_s| = 2$ transition. Since the line shape of the high- and low-field H_z absorptions of the $|\Delta m_s| = 1$ region was unchanged upon temperature variation, however, we used both the half-field transition and the outer $|\Delta m_s| = 1$ absorptions for the temperature dependent EPR measurement in rigid solution of MTHF (Figure 5A). The temperature dependence of signal intensities is shown in Figure 5B. Two major findings could be made thereby: (i) the intensities of both $|\Delta m_s| = 1$ and $|\Delta m_s| = 2$ signals reach a maximum at about 20 K, which is in accordance with a thermally excited triplet state that becomes populated above 5 K, and (ii) the orthorhombicity

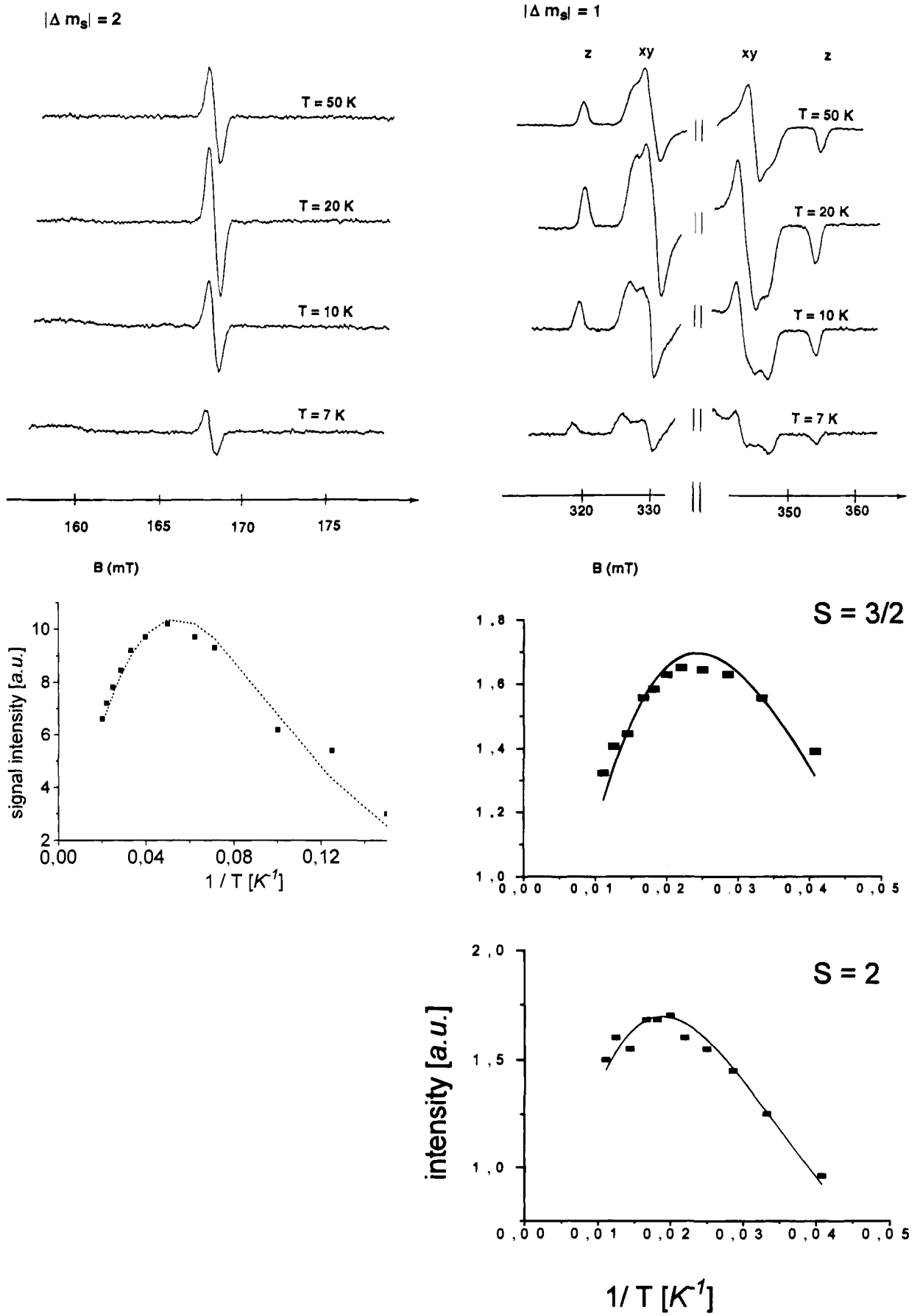

Figure 5. Temperature dependence of the signal intensity (au) for the $|\Delta m_s| = 2$ and $|\Delta m_s| = 1$ transitions of $2^{2\bullet-}/2K^+$ in MTHF: (A, top) EPR spectra of the $|\Delta m_s| = 2$ and $|\Delta m_s| = 1$ absorptions of $2^{2\bullet-}/2K^+$ at different temperatures; (B, bottom left) Curie plot of the signal intensity of the $|\Delta m_s| = 1$ transition vs the reciprocal absolute temperature, the solid line being a simulation curve with an S−T energy gap of 60 cal/mol (see text); (C, bottom right) Curie plots of the signal intensities of the $|\Delta m_s| = 1$ transitions for $\mathbf{3a}^{3\bullet-}$ ($S = 3/2$) and $\mathbf{4}^{4\bullet-}$ ($S = 2$) vs reciprocal temperature.

increases upon lowering the temperature from 100 to 10 K, with clean separation of x and y components at lowest temperature.

The curve of EPR intensity versus $1/T$ were fitted with the intensity function $I = (C/T)\exp(-\Delta E_{s-t}/RT)/(1 + 3\exp(-\Delta E_{s-t}/RT))$,[42] resulting in a singlet−triplet energy separation of $\Delta E = 60$ cal/mol. The thermal behavior was reversble for all temperatures examined, and no significant change of D values was observed. A possibility of saturation in intensity was excluded by careful control of microwave power dependence on intensities. Thus, the observed triplet is unequivocally the thermally excited state.

From the inequivalence of the x and y components changed D and E parameters were evaluated from the spectra with zero-field splitting D at 20 K, then being $D = 17.0$ mT (159×10^{-4} cm^{-1}), and the asymmetry component E determined to be 0.9 mT (8.4×10^{-4} cm^{-1}). Consequently, a symmetry reduction at low temperatures takes place, which is caused by a twisting of the anthracene subunits to less than ca. 80°. This angle in the charged state is then very similar to the twisting angle of **3b** from X-ray structural analysis, where an angle $\theta = 75°$ was found.[23]

Magnetic susceptibility measurements of $\mathbf{2}^{2\bullet-}$ in rigid solution of MTHF and of a powder sample of $\mathbf{2}^{2\bullet-}$ obtained by evaporation of the solvent also confirm a singlet−triplet transition with a maximum of signal heights at 20 K.[24] This method, on the other hand, measures the bulk magnetization, where monoradical centers and solvent molecules lead to a paramagnetic background, such that the signal decrease due to partial spin pairing is more difficult to extract.

Since the singlet−triplet excitation energy is very small for $\mathbf{2}^{\bullet-}$, we also measured the signal intensity for the higher spin states in $\mathbf{3}^{3\bullet-}$ and $\mathbf{4}^{4\bullet-}$. Despite the hope for larger stability of the higher spin states, the temperature dependent EPR signal intensity yielded maxima at around 40 and 60 K, respectively. The curves were fitted for doublet to quartet transition ($S = 3/2$; $I = (C/T)\exp(\Delta E_{d-qua}/_RT)/(2 + 4\exp(\Delta E_{d-qua}/RT))$ and for quintet to singlet transition ($S = 2$; $I = (C/T)\exp(\Delta E_{s-quin}/RT)/(1 + 3\exp(\Delta E_{t-quin}/RT) + 5\exp(\Delta E_{s-quin}/RT))$.[42] Thereby thermal excitation energies by $\Delta E_{d-qua} = 120$ cal/mol for the $S = 3/2$ state and $\Delta E_{s-quin} = 180$ cal/mol for the $S = 2$ state could be evaluated from the experimental data (Figure 5C). It thus seems that still more rigid alignment between the anthracenes would be necessary, e.g., by additional substituents in the 1,8-positions and 1′,8′-positions.

3. Conclusion

For 9,10-anthrylenes, a relationship exists between formation of higher spin states in polyradicals, and effective localization versus delocalization of spin density in monoradical anions. The intramolecular electron transfer in monocharged species of oligo(9,10-anthrylene)s between anthracene moieties sensitively depends on the special substitution pattern, on the radical concentration, and thus on the ion pair conditions (SSIP, CIP). It is possible to control localization/delocalization in 9,10-anthrylenes by changing the way of substitution and the polarity of the solution and thereby the ion pairing. This finding demands particular attention since intramolecular electron transfer has been recently considered as a background process of intramolecular electronics.[43]

The trianion of **3a** and the tetraanion of **4**, on the other hand, are found in a quartet state and a quintet state at ambient temperatures, respectively. The highly charged species of **2**, **3a**, and **4** and the polymer are remarkably stable, and we have found that samples in evacuated probe tubes can be stored at 278 K for up to several months without loss in the intensity of the EPR signals. Thus, these molecules are part of only a handful of organic polyradicals, which are stable at moderate temperatures. Since the charged 9,10-anthrylenes carry charges, they obviously tend less to coupling reactions than do the well-studied neutral radicals, and are therefore chemically more stable. Although the higher spin state formation of $\mathbf{2}^{2\bullet-}/2K^+$, $\mathbf{3a}^{3\bullet-}/3K^+$, and $\mathbf{4}^{4\bullet-}/4K^+$ follows our arguments based on orthogonal alignment by steric hindrance, temperature dependent EPR measurements reveal that the ground states are still low spin with very small energetic separation to the high spin states. As found for $\mathbf{2}^{2\bullet-}/2K^+$ the ground state singlet is due to deviation from orthogonality; thus, even stronger limitation of rotational freedom between the anthracenes seems to be important. These structural variations and magnetic studies will have to include a search for suitable solvents and counterions for the polymeric material in order to generate high-spin material in solution.

4. Experimental Section

Alkali Metal Reductions. To prepare potassium and lithium organic compounds special glass tubes were used, which could be connected to a vacuum line. Dried (stirred over Na/K alloy) and degassed solvent (MTHF, THF or THF-d_8) was condensed on the compound. Alkali metal was transferred into the reduction cell, which in turn was connected to a NMR or EPR tube, respectively. The tube was sealed off and the solution carefully degassed under vacuum. When the tube was turned down, the solution was brought into contact with the metal at low temperature. This reduction process is then controlled by NMR, UV/vis, and EPR spectroscopy.

EPR Measurement. The reported EPR/ENDOR spectra were obtained on a Bruker ESP-300 EPR/ENDOR spectrometer equipped with a field frequency lock, a variable temperature accessory, and a data acquisition system. All precautions were taken to avoid undesirable spectral line broadenings, such as those arising from microwave power saturation and magnetic field overmodulation. Sample solutions were prepared as described above.

General Methods: melting points, Büchi Dr. Tottoli apparatus (uncorrected); commercial solvents purified according to standard procedures; IR spectra, Nicolet FT-IR 320 spectrometer; ^1H and ^{13}C NMR spectra, Varian Gemini 200, Bruker AC 300, Bruker AMX 500 spectrometers; MS (EI), VG Instruments ZAB-2 spectrometer; MS (FD), Finnigan MAT 95 spectrometer; elemental analysis, Department of Chemistry and Pharmacy of the University of Mainz; column chromatography, glass columns packed with silica gel (70−320 mesh) with eluants specified below; electrochemical measurements, cyclic voltammograms measured with an apparatus and under conditions as described previously,[2] ferrocene used as an internal standard (310 mV versus SCE) for calibration.

10-Bromo-9,9′-bianthryl (2a). At 0 °C a solution of bromine (1.36 g, 0.0085 mol) in CCl_4 (200 mL) was added dropwise over 20 h to a solution of **2** (3.01 g, 0.0085 mol) in CCl_4 (250 mL). The mixture was allowed to react for a further 4 h at room temperature. After concentration of the reaction mixture, the organic phase was washed repeatedly with 2 N NaOH and water and dried ($MgSO_4$), and finally the solvent was removed. Column chromatography on silica gel (petroleum ether/methylene chloride, 10:1) gave 1.3 g (40%) of pure **2a**. Mp: 272 °C dec. ^1H NMR (200 MHz, $CDCl_3$): δ 7.01−7.19 (m, 8 H, H-1,1′,2,2′,7,7′,8,8′), 7.39−7.47 (m, 2 H, H-3′,6′), 7.51−7.59 (m, 2 H, H-3,6), 8.13 (d, $J = 8.3$ Hz, 2 H, H-4′,5′), 8.67 (s, 1H, H-10′), 8.69 (d, $J = 8.8$ Hz, 2 H, H-4,5). EI-MS (70 eV): *m/e* 434 (100, $M^+ + 1$), 433 (27, M^+), 432 (99, $M^+ - 1$).

10,10′-Dibromo-9,9′-bianthryl (2b). At 0 °C a solution of bromine (1.8 g, 0.0112 mol) in CCl_4 (100 mL) was added dropwise over 2 h to a solution of **2** (1.8 g, 0.0051 mol) in CCl_4 (100 mL). After 24 h of further reaction time, the reaction mixture was concentrated and the crude product precipitated with ethanol. Recrystallization afforded 2

(42) Breslow, R.; Chang, H. W.; Hill, R.; Wasserman, E. *J. Am. Chem. Soc.* **1967**, *89*, 1112.
(43) Joachim, C.; Launay, J. P. *J. Mol. Electron.* **1990**, *6*, 37.

g (76%) of **2b**. ^{1}H NMR (200 MHz, $CDCl_3$): δ 8.73 (d, J = 8.9 Hz, 4 H, H-4,4′,5,5′), 7.59 (dt, J = 1.5 Hz, 7.3 Hz, 4 H, H-3,3′,6,6′), 7.40 (m, 8 H, H-1,1′,2,2′,7,7′,8,8′). EI-MS (70 eV): *m/e* 515 (20, M^+ + 3), 514 (54, M^+ + 2), 513 (34, M^+ + 1), 512 (100, M^+), 352 (42, M^+ − 2Br).

10-Cyano-9,9′-bianthryl (2c). A mixture of **2b** (1 g, 0.0023 mol), CuCN (0.3 g, 0.0032 mol), and freshly distilled dimethylformamide (150 mL) was refluxed for 5 h under an inert atmosphere. After cooling to room temperature, the reaction mixture was poored into diluted $FeCl_3$ solution (500 mL, 1 M in water), extracted with $CHCl_3$, and dried ($MgSO_4$), and then the solvent was removed. The crude product was purified by recrystallization from $CHCl_3$/methanol (1:1) and column chromatography on silica gel (chloroform/petroleum ether, 2:1) to give a yellow-green powder of **2c**. Yield: 0.53 g (60%). ^{1}H NMR (200 MHz, $CDCl_3$): δ 8.77 (s, 1 H, H-10′), 8.63 (d, J = 8.8 Hz, 2 H, H-4,5), 8.20 (d, J = 8.4 Hz, 2 H, H-4′,5′), 7.72 (m, 2 H, H-3,6), 7.50 (m, 2 H, H-3′,6′), 7.24 (m, 6 H, H-1,2,2′,7,7′,8), 7.01 (d, J = 8.7 Hz, 2 H, H-1′,8′). EI-MS (70 eV): *m/e* 379 (100, M^+), 175 (37, anthryl cation). Anal. Calcd for $C_{29}H_{17}N$: C, 91.78; H, 4.52. Found: C, 91.91; H, 4.61.

10,10′-Dicyano-9,9′-bianthryl (2d). A suspension of **2b** (2 g, 0.0039 mol), CuCN (1 g, 0.0112 mol), and freshly distilled quinoline (200 mL) was refluxed for 3 h under an inert atmosphere. After cooling to room temperature, the mixture was poored into diluted $FeCl_3$ solution (500 mL, 1 M in water), repeatedly extracted with chloroform, and dried ($MgSO_4$). After removal of the solvent, the residue was chromatographed on silica gel (petroleum ether/methylene chloride, 1:2) to afford 0.5 g (32%) of **2d**. ^{1}H NMR (200 MHz, $CDCl_3$): δ 8.64 (dd, J = 0.8 Hz, 8.7 Hz, 4 H, H-4,4′,5,5′), 7.74 (m, 4 H H-3,3′,6,6′), 7.31 (m, 4 H, H-2,2′,7,7′), 7.09 (dd, J = 0.8 Hz, 8.8 Hz, 4 H, H-1,1′,8,8′). ^{13}C NMR (50 MHz, $CDCl_3$): δ 138.8 (C-9,9′), 133.5, 131.1, 129.5, 127.9, 127.6, 126.4, 118.5 (*C*−CN), 107.1 (C−*C*N). EI-MS (70 eV): *m/e* 404 (100, M^+), 402 (11, M^+ − 2), 378 (14, M^+ − CN). Anal. Calcd for $C_{30}H_{16}N_2$: C, 89.09; H, 3.99. Found: C, 88.89; H, 4.04.

2′,3′-Dihexyl-9,10-trianthrylene (3a). To a suspension of **6a** (15.42 g, 0.06 mol) in absolute diethyl ether (400 mL) at 0 °C was added 41.6 mL of *n*-butyllithium (1.6 M in hexane). After stirring the mixture for 15 min at 0 °C, a solution of **5a** (7.56 g, 0.02 mol) in absolute diethyl ether (100 mL) was added dropwise. The mixture was allowed to stir for 72 h, and then the reaction was quenched with 10 mL of acetic acid and the ether removed. The residue was dissolved in acetic acid (300 mL) under argon. Finally, 40 mL of H_3PO_2 (aqueous solution, 50%) and 5 mL of HI (aqueous solution, 57%) were added. The reaction mixture was kept for 2 h at 80 °C. After cooling to room temperature, the yellow precipitate was filtered and purified by column chromatography (petroleum ether/methylene chloride, 5:1) to afford 8.3 g (60%) of **3a**. ^{1}H NMR (200 MHz, $C_2D_2Cl_4$): δ 8.74 (s, 2 H, H-10′,10″), 8.26−8.18 (m, 4 H, H-4,5,4″,5″), 7.56−7.50 (m, 4 H, H-3,6,3″,6″), 7.46−7.24 (m, 8 H, H-1,2,7,8,1″,2″,7″,8″), 7.22−7.00 (m, 4 H, H-5′,6′,7′,8′), 6.95 (s, 2H, H-1′,4′), 2.35 (t, 4 H, J = 7.8 Hz, α-benzylic H), 1.25−0.8 (m, 16 H, CH_2), 0.71 (t, 6 H, J = 6.3 Hz, CH_3). ^{13}C NMR (50 MHz, $CDCl_3$): δ 140.3 (C-2′,3′), 134.4 (q), 133.0 (q), 132.3 (q), 132.2 (q), 131.6 (q), 131.2 (q), 129.1 (t), 127.7 (t), 127.6 (t), 126.3 (t), 126.2 (t), 125.8 (t), 125.6 (t), 33.0 (CH_2), 31.9 (CH_2), 30.7 (CH_2), 29.2 (CH_2), 22.9 (CH_2), 14.5 (CH_3). EI-MS (70 eV): *m/e* 698 (100, M^+), 329 (87, M^+ − 2anthryl − CH_3), 177 (43, anthryl cation). Anal. Calcd for $C_{54}H_{50}$: C, 91.79; H, 7.21. Found: C, 92.67; H, 7.30.

2,2′,2″,6,6′,6″-Hexa-*tert*-butyl-9,10-trianthrylene (3b). A solution of **5b** (4.2 g, 0.0132 mol) in absolute diethyl ether (200 mL), a suspension of **6e** (10 g, 0.026 mol) in absolute diethyl ether (100 mL), 16.5 mL (0.026 mol) of *n*-butyllithium (1.6 M in hexane), 10 mL of acetic acid, and a mixture of 30 mL of H_3PO_2 (aqueous solution, 50%), 2 mL HI (aqueous solution, 57%, and acetic acid (250 mL) were allowed to react as described for **3a**. The crude product was then purified by recrystallization from ethanol and column chromatography on silica gel (petroleum ether/methylene chloride, 10:1) to give 3.9 g (66%) of **3b** (two atropisomers). Mp: 280 °C dec. By further chromatography on silica gel (petroleum ether/methylene chloride, 20:1), the atropisomers of **3b** could be separated in small quantities for spectroscopic studies. ^{1}H NMR (200 MHz, $CDCl_3$): δ 0.96 (s, 18 H, $C(CH_3)_3$), 1.15 (s, 18 H, $C(CH_3)_3$), 1.49 (s, 18 H, $C(CH_3)_3$, 7.17−7.32 (m, 12 H, H-1,1′,1″,3′,4′,5′,7,7′,7″,8,8′,8″), 7.61 (dd, 2 H, J = 8.9 Hz, 1.4 Hz, H-3,3″), 8.08 (d, 2 H, J = 1.4 Hz, H-5,5″), 8.13 (d, 2 H, J = 8.9 Hz, H-4,4″), 8.64 (s, 2 H, H-10,10″). ^{13}C NMR (50 MHz, $CDCl_3$) (mixture of two atropisomers): δ 30.5 (p, $C(CH_3)_3$), 30.6 (p, $C(CH_3)_3$), 30.8 (p, $C(CH_3)_3$), 30.9 (p, $C(CH_3)_3$), 34.5 (q, $C(CH_3)_3$), 34.7 (q, $C(CH_3)_3$), 3.48 (q, $C(CH_3)_3$), 121.6 (t), 122.4 (t), 122.6 (t), 124.3 (t), 124.4 (t), 124.9 (t), 125.1 (t), 126.1 (t), 126.2(t), 126.9 (t), 127.1(t), 128.0 (t), 128.1 (t), 130.0 (q), 130.2 (q), 130.3 (q), 130.4 (q), 130.6 (q), 130.8 (q), 130.9 (q), 131.2 (q), 131.4 (q), 132.8 (q), 133.0 (q), 146.7, 146.8, 146.9, 147.1, 147.2 (q, C-2,2′,2″,6,6′,6″). FD-MS: *m/e* 870 (11, M^+ + 2), 869 (41, M^+ + 1), 868 (79, M^+), 867 (100, M^+), 867 (100, M^+ − 1). Anal. Calcd for $C_{66}H_{74}$: C, 91.40; H, 8.60. Found: C, 91.51; H, 8.67.

2,2‴,3,3‴-Tetrahexyl-9,10-tetraanthrylene (4). To a solution of **6c** (0.75 g, 2.0 × 10^{-3} mol) in absolute diethyl ether (100 mL) at 0 °C under argon was added 1.15 mL of *n*-butyllithium (1.6 M in hexane). The mixture was stirred for 15 min, and then a suspension of **8** (353 mg, 9.2 × 10^{-4} mol) in absolute diethyl ether (100 mL) was added dropwise. After stirring for 24 h, the reaction was quenched with 10 mL of glacial acetic acid and the ether removed. The residue was dissolved in acetic acid (100 mL), treated with 10 mL of H_3PO_2 (aqueous solution, 50%) and 1.5 mL at HI (aqueous solution, 57%), kept for 2 h at 80 °C, and finally cooled to room temperature. The yellow precipitate was purified by recrystallization from methylene chloride/hexane (1:1) and chromatography on silica gel (petroleum ether/methylene chloride, 5:1). Yield: 260 mg (31%) of **4**. ^{1}H NMR (200 MHz, $C_2D_2Cl_4$): δ 8.67 (s, 2 H, H-10), 8.21 m, 2 H, H-5), 7.99 (s, 2 H, H-4), 7.60−7.15 (m, 22 H, H-6,7,8,1′−8′), 7.03 (s, 2 H, H-1), 2.83 (t, J = 7.2 Hz, 4 H, α-benzylic H), 2.61 (t, J = 7.02 Hz, 4 H, α-benzylic H), 1.80−0.94 (m, 38 H, CH_2, CH_3), 0.67 (t, J = 5.8 Hz, 6 H, CH_3). ^{13}C NMR (50 MHz, $CDCl_3$): δ 140.3, 140.2 (q, C-2,3), 135.0 (q), 134.4 (q), 132.6 (q), 132.2 (q), 132.1 (q), 132.0 (q), 131.9 (q), 131.8 (q), 131.5 (q), 129.1 (t), 128.0 (t), 127.9 (t), 127.8 (t), 127.5 (t), 127.4 (t), 127.3 (t), 126.6 (t), 126.4 (t), 126.3 (t), 126.2 (t), 126.1 (t), 126.0 (t), 125.7 (t), 125.4 (t), 33.4 (s, CH_2), 33.1 (s, CH_2), 32.4 (s, CH_2), 32.0 (s, CH_2), 31.2 (s, CH_2), 30.1 (s, CH_2), 30.0 (s, CH_2), 29.1 (s, CH_2), 23.2 (s, CH_2), 22.9 (s, CH_2), 14.6 (p, CH_3), 14.4 (p, CH_3). FD-MS: *m/e* 1043 (100, M^+), 1044 (82, M^+ + 1), 1045 (36, M^+ + 2). Anal. Calcd for $C_{80}H_{82}$: C, 92.08; H, 7.92. Found: C, 92.29; H, 7.81.

2′,3′-Dihexyl-9,10-trianthrylene Hexaanion ($3a^{6-}/Li^+$). A solution of **3a** (6 mg) in 2 mL of THF-d_8 was contacted for one week at 250 K with lithium metal to give a deep blue solution of $3a^{6-}/6Li^+$. ^{1}H NMR (500 MHz, THF-d_8) (signals were assigned with the aid of a H,H correlated 2D spectrum: δ 4.78 (s, 2 H, H-7′,8′), 4.39 (s, 4 H, H-2,2″,7,7″), 4.19 (s, 4 H, H-3,3″,6,6″), 3.98 (s, 2 H, H-4′,8′), 3.55 (s, 2 H, H-1′,4′), 3.42 (s, 4 H, H-1,1″,8,8″), 3.06 (s, 4 H, H-4,4″,5,5″), 1.73 (m, 4 H, α-benzylic H), 1.58 (s, 2 H, H-10,10″), 1.45−1.25 (m, 16 H, CH_2), 0.95−0.85 (m, 6 H, CH_3). ^{13}C NMR (125 MHz, THF-d_8): δ 155.8 (q), 149.1 (q), 148.8 (q), 148.2 (q), 128.5 (q), 119.3 (t), 119.0 (t), 117.6 (t), 105.1 (t), 104.7 (t), 103.7 (t), 101.4 (t) 98.0 (t), 81.8 (q), 79.7 (q), 77.6 (t), 34.8 (s, CH_2), 34.7 (s, CH_2), 33.7 (s, CH_2), 33.0 (s, CH_2), 25.4 (s, CH_2), 16.3 (p, CH_3).

Quenching of $3a^{6-}/6Li^+$. To quench the highly charged anion, the NMR tube was opened in a silicon skin filled with argon. The necessary reagent (dimethyl sulfide) was injected. After disappearance of the color, the solution was stirred for half an hour, and 10 mL of water was added. The organic layer was dried ($MgSO_4$) and concentrated. The product was filtered with $CHCl_3$ through a pipet filled with silica gel and evaporated. To characterize the product, FD mass spectroscopy was used. The incorporation of six methyl groups in the substrate is proved by detection of a peak at 788 D and provides evidence for the number of six extra electrons in the ion.

Acknowledgment. We gratefully thank Professor Dr. K. Müllen and Professor Dr. N. Tyutyulkov for many helpful discussions and the MPG and VW-Stiftung for financial support.

JA950633R